核内核子の一粒子運動の基礎と密度汎関数理論

中務　孝

- 核内での核子の1粒子運動
  - 実験データ
- 簡単な平均場模型での解析
  - 実験データとの矛盾
- 密度汎関数理論
  - アプリケーション

2011.8.5 サマースクール「クォークから超新星爆発まで」

コーン･シャム方程式

- “1粒子”方程式

$$h[\rho]|\phi_i\rangle = \varepsilon_i|\phi_i\rangle$$

- 正当化
  - Hohenberg-Kohn 定理
  - 時間依存版：Runge-Gross 定理
  - Kohn-Sham スキーム

$$E[\rho] \Rightarrow \quad h[\rho]|\phi_i\rangle = \varepsilon_i|\phi_i\rangle$$

$$h[\rho] \equiv \frac{\delta E}{\delta \rho}$$

- 平均場との相違
  - 原子核の飽和性との矛盾を解消

Three major faces of nuclei

Liquid

Gas

Chaos

Evidence of the single-particle motion

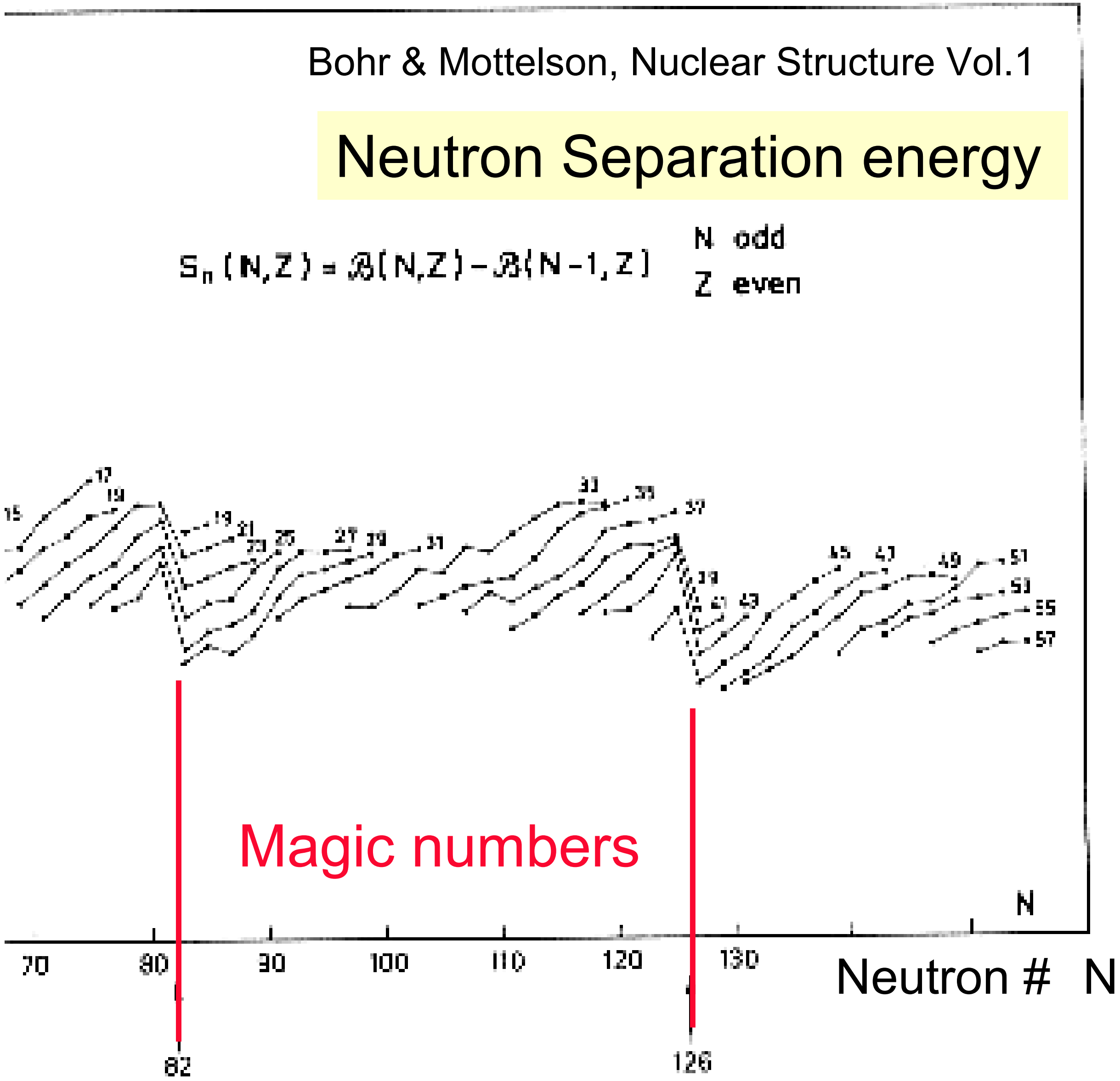

Shell Model
(Mayer-Jensen)

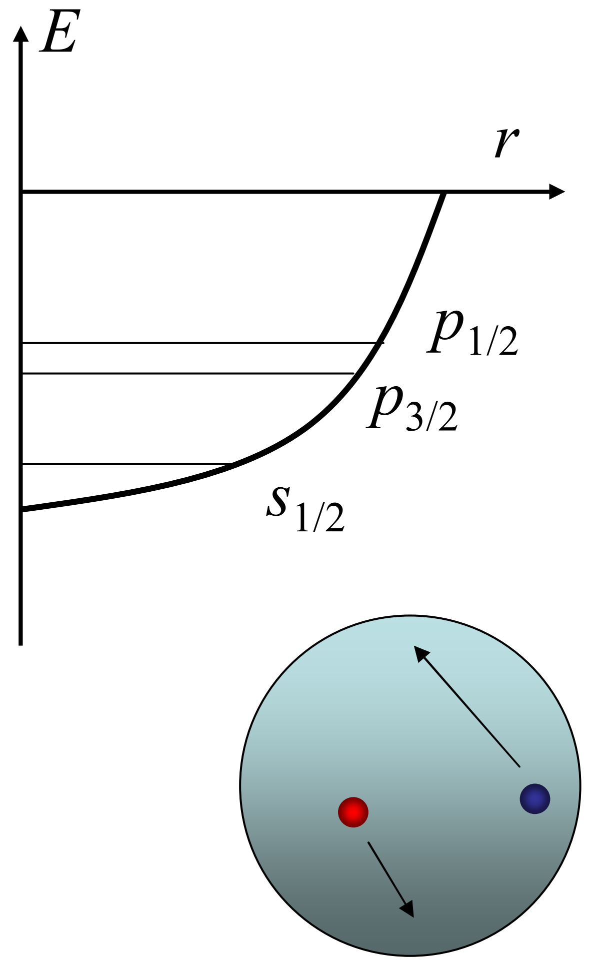

Energy required to remove two neutrons from nuclei

(2-neutron binding energies = 2-neutron “separation” energies)

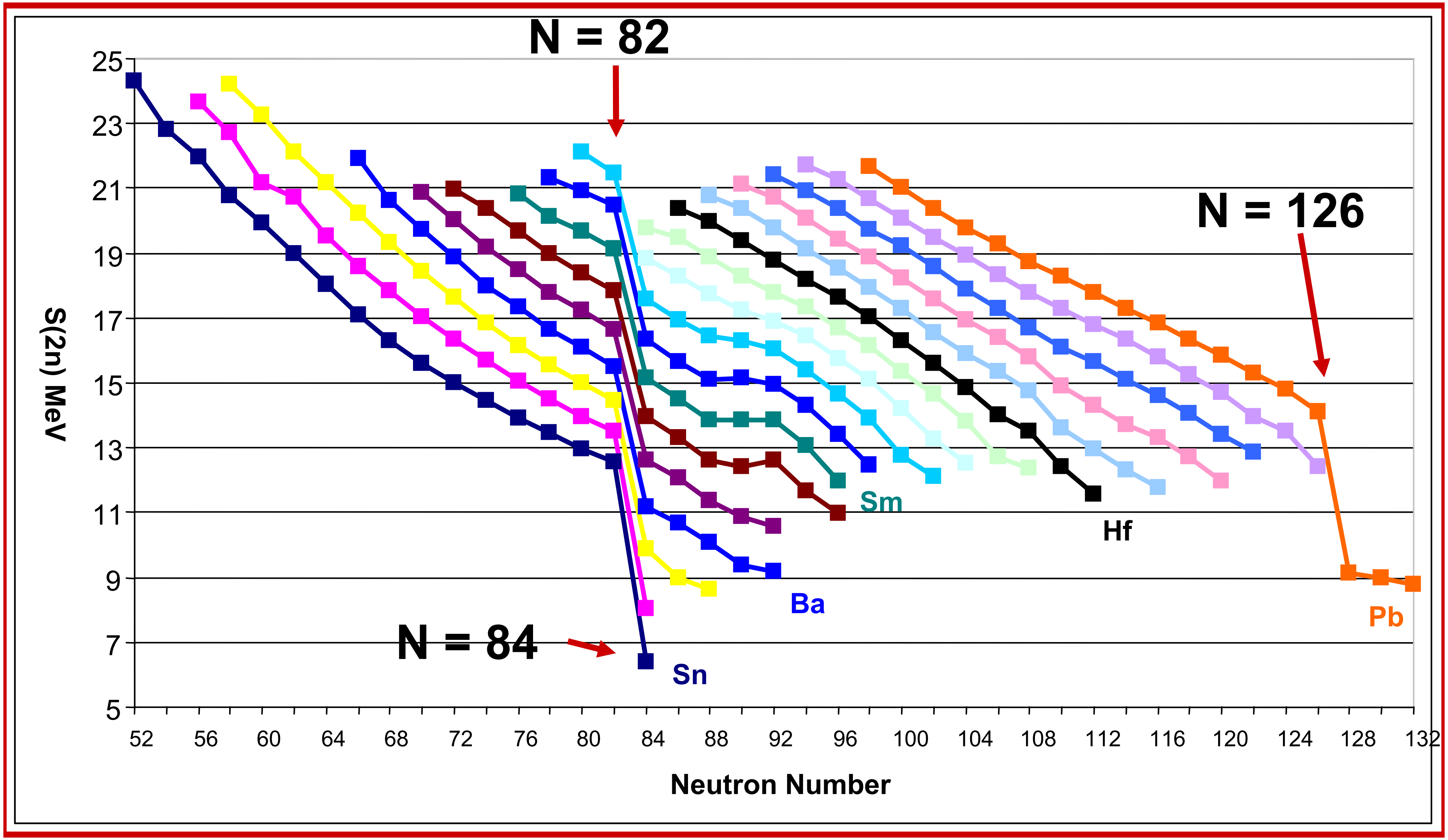

From a lecture by R. Casten

Mayer-Jensen's Shell Model

Harmonic oscillator potential + spin-orbit force

$$V(r) = \frac{1}{2} M\omega^2 r^2 + v_{ll}\ell^2 + v_{ls}\vec{\ell}\cdot\vec{s}$$

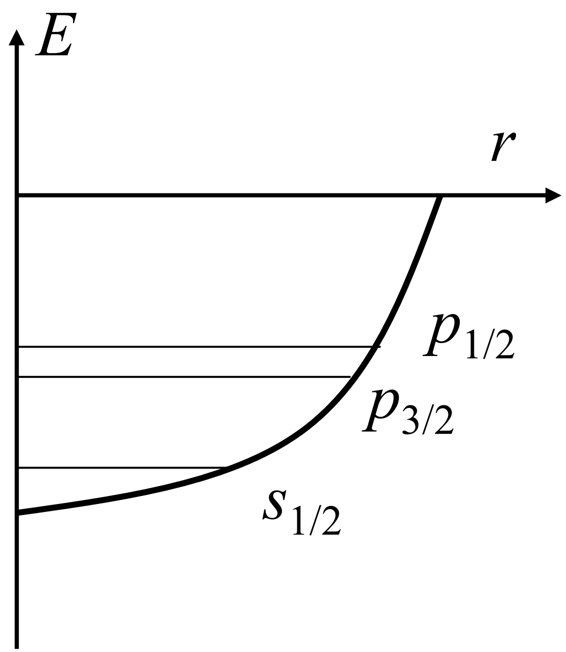

→ Correct magic numbers:

(N,Z)=2, 8, 20, 28, 50, 82, 126

"Gas"-like picture for nucleus

$$\lambda >> R$$

Spin-parity of odd nuclei

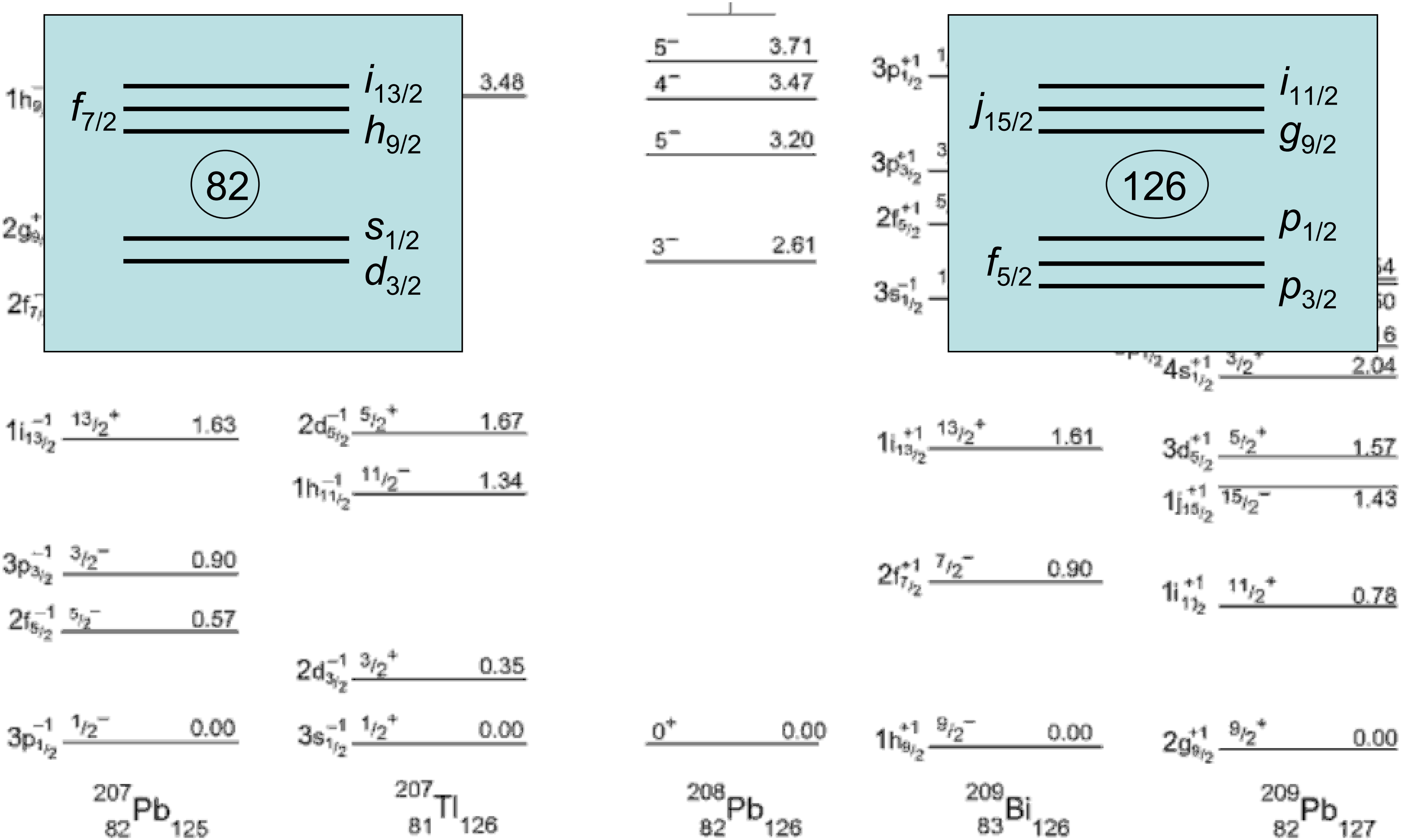

Neutron scattering cross section

From Bohr and Mottelson,
Nuclear Structure Vol.1

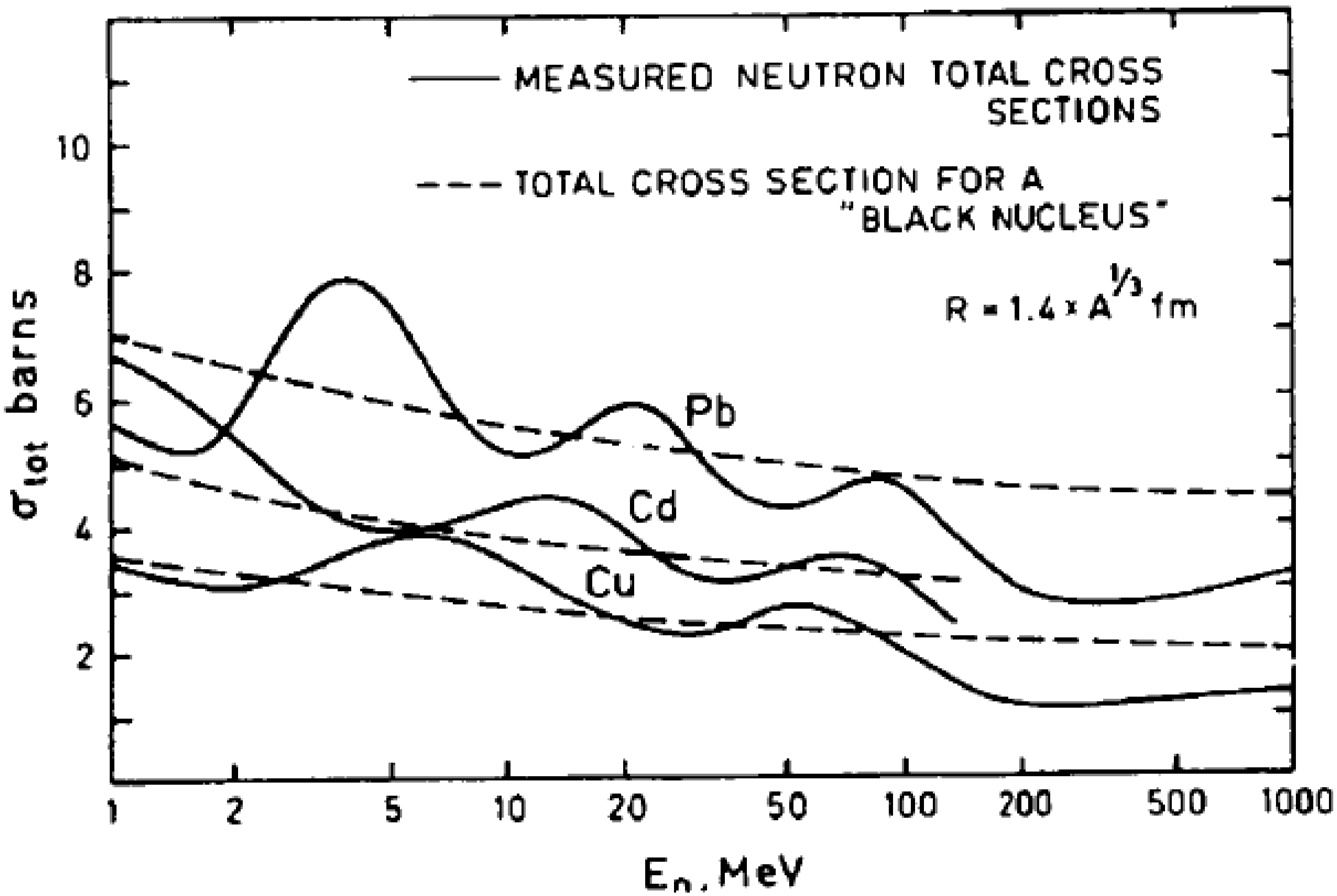

Phase shift & optical theorem

Phase shift

$$\delta(k) \approx 2\left(k_{in} - k\right)R$$

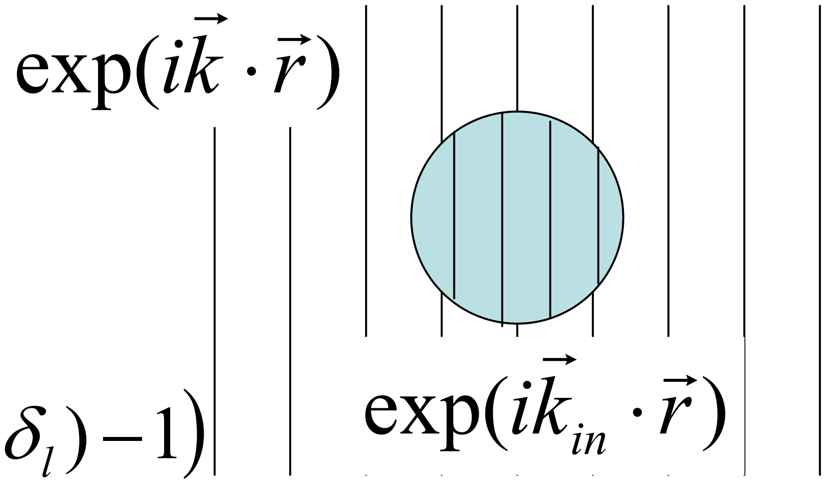

Scattering amplitude

$$f(\theta) = \frac{1}{2ik}\sum_l \left(2l+1\right)\left(\exp(2i\delta_l) - 1\right)$$

$$\eta_l = \exp(2i\delta_l), \quad \left|\eta_l\right| = 1$$

Total cross section

$$\sigma_{tot} = \frac{4\pi}{k}\,\mathrm{Im}\, f(\theta) = \frac{4\pi}{k^2}\sum_l \left(2l+1\right)\sin^2\delta_l$$

→ Oscillation as a function of energy

cf) Ramsauer-Townsend effect

Nuclear transparency

Optical potential

$$V + iW \Rightarrow k_{in} + \frac{i}{2\lambda}$$

Complex phase shift

$$\eta_l = \exp(2i\delta_l), \quad |\eta_l| \leq 1$$

Total cross section

$$\sigma_{tot} = \frac{4\pi}{k}\,\mathrm{Im}\, f(\theta) = \frac{2\pi}{k^2}\sum_l (2l+1)(1-\mathrm{Re}\,\eta_l)$$

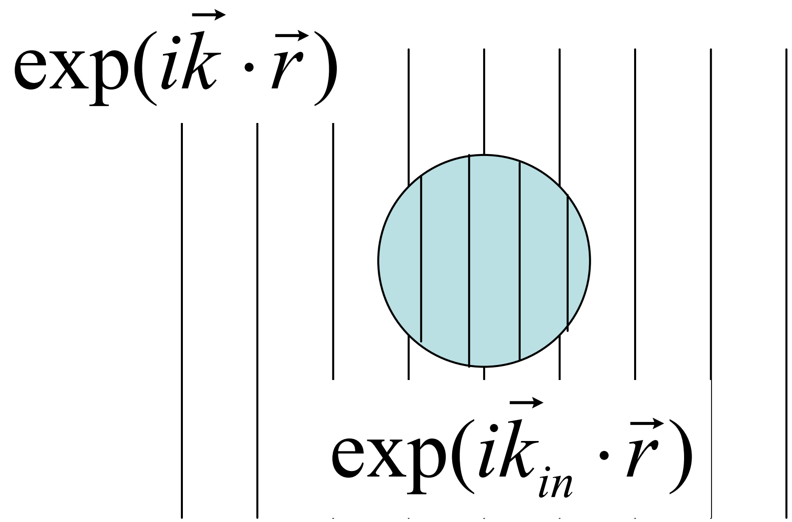

Oscillation frequency → Real part: V

Oscillation amplitude → Imaginary part: W → Mean free path: λ

$$-V \approx 50 - 0.3E, \quad -W \approx (0 \sim 2) + 0.1E$$ in units of MeV

$$\Rightarrow \quad \lambda \approx \alpha R\,, \quad [\alpha \approx 1 \sim 10 \text{ or more}]$$

Energy dependence of the imaginary part

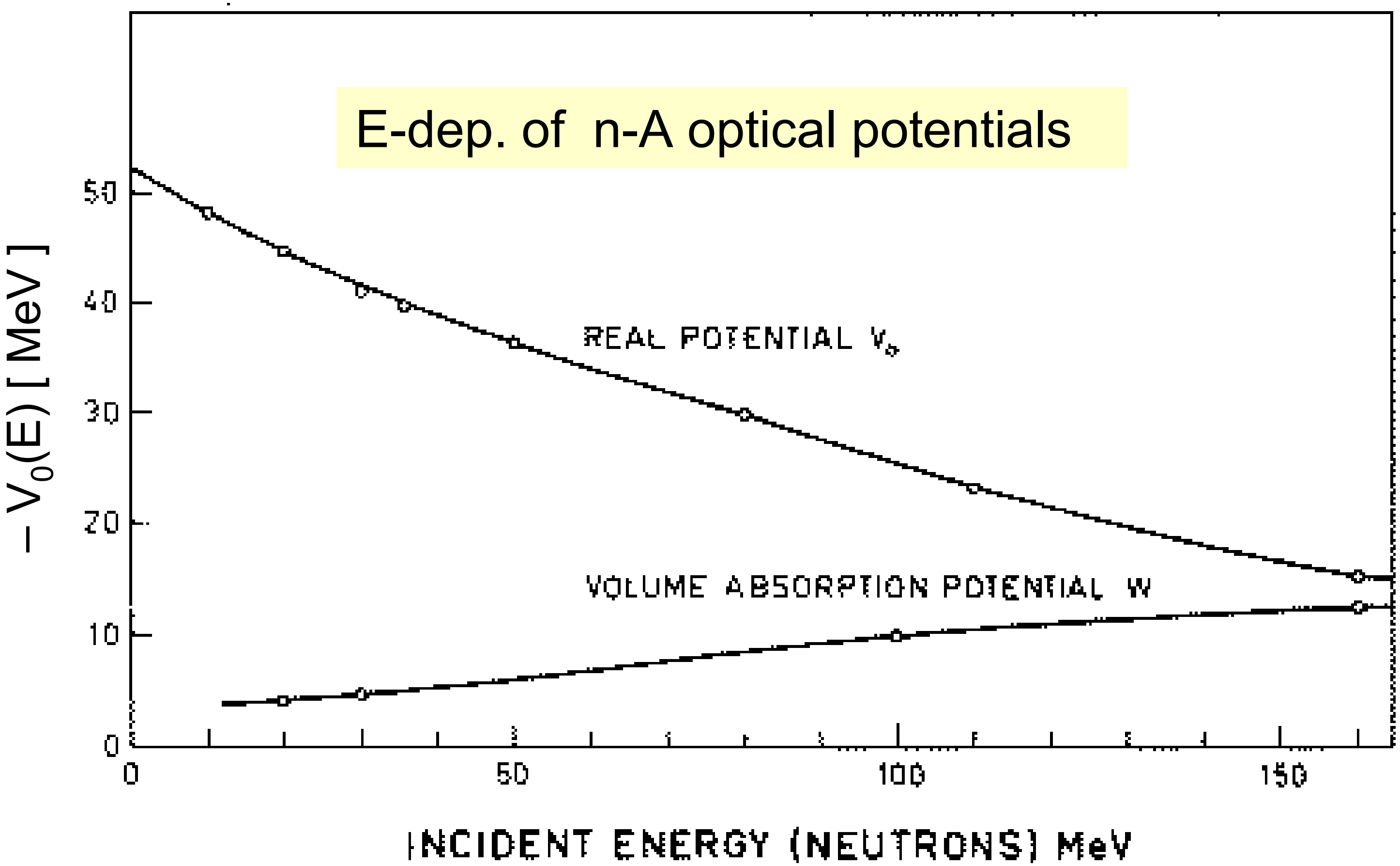

The imaginary potential becomes smaller for lower-energy neutrons.

“Gas” picture

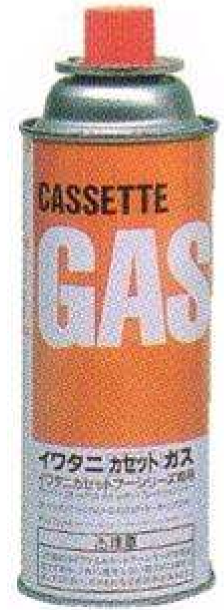

Success of the shell model

$$V(r) = \frac{1}{2} M\omega^2 r^2 + v_{ll}\ell^2 + v_{ls}\vec{\ell}\cdot\vec{s}$$

and

Optical model analysis for neutron scattering

suggest “gas” picture of the nucleus

$$\lambda >> R$$

Is this consistent with other aspects of nuclei?

Nuclear Saturation

The most basic property of nucleus

B/A ~ 8 MeV

(B/A ~ 16 MeV for nuclear matter)

Density $\rho \approx 0.16\ \mathrm{fm}^{-3}$

Liquid drop model

Bethe-Weizsäcker mass formula

$$B(N,Z) = a_V A - a_S A^{2/3} - a_{sym}\frac{(N-Z)^2}{A} - a_C \frac{Z^2}{A^{1/3}} + \delta(A)$$

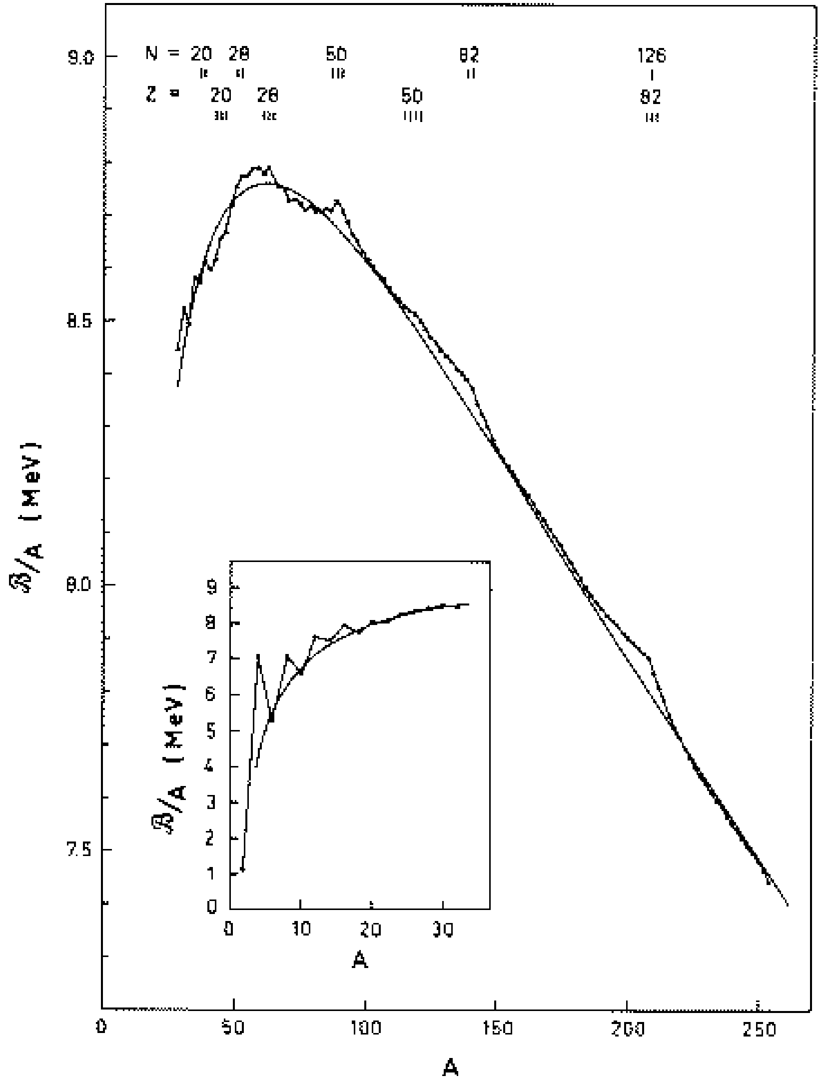

Saturation properties of nuclear matter

- Symmetric nuclear matter w/o Coulomb
  - $N = Z = A/2$
- Constant binding energy per nucleon
  - Constant separation energy

  $$B/A \approx S_{n(p)} \approx 16\,\mathrm{MeV}$$
- Saturation density

  $$\rho \approx 0.16\,\mathrm{fm}^{-3} \quad \Rightarrow \quad k_F \approx 1.35\,\mathrm{fm}^{-1}$$
  - Fermi energy

  $$T_F = \frac{\hbar^2 k_F^2}{2m} \approx 40\,\mathrm{MeV}$$

Mean-field picture of the nucleus

- Mean-field model

$$h[\rho]|\phi_i\rangle = \varepsilon_i|\phi_i\rangle \qquad i\frac{\partial}{\partial t}|\psi_i(t)\rangle = h[\rho(t)]|\psi_i(t)\rangle$$

- Is this consistent with the saturation property?
  – Analysis with a simple potential model for nuclear matter

$$h = -\frac{\hbar^2}{2m}\nabla^2 + V$$

A constant mean-field potential

- Separation energy

$$S = -\left(T_F + V\right), \quad V \approx -55\,\mathrm{MeV}$$

- Binding energy in the mean field

$$-B = \sum_{i=1}^{A}\left(T_i + \frac{V}{2}\right), \quad T_i = \frac{\hbar^2 k_i^2}{2m}$$

$$= A\left(\frac{3}{5}T_F + \frac{V}{2}\right)$$

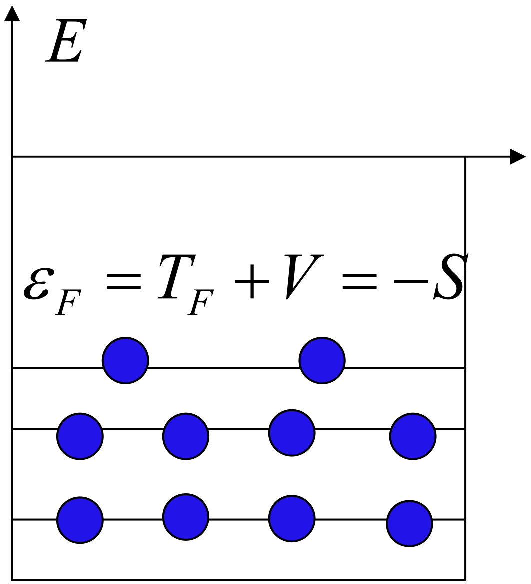

- $S = {}^{B}\!/_{A} \quad \Rightarrow T_F = -\frac{5}{4}V$

Inconsistent with nuclear binding

Momentum-dependent potential

- State-dependent potential

$$V_F = \langle V \rangle + {T_F}/{5} + {B}/{A}$$

  - The potential becomes shallower for particles with a weaker binding
- Momentum dependence
  - The lowest order → "Effective mass"

$$V = U_0 + U_1 k^2 \quad \Rightarrow {m^*}/{m} = \left(1 + {U_1 k_F^2}/{T_F}\right)^{-1}$$

$$= \left(\frac{3}{2} + \frac{5}{2}\frac{B}{A}\frac{1}{T_F}\right)^{-1} \approx 0.4$$

Nucleons’ effective mass

Energy dependence of optical potential

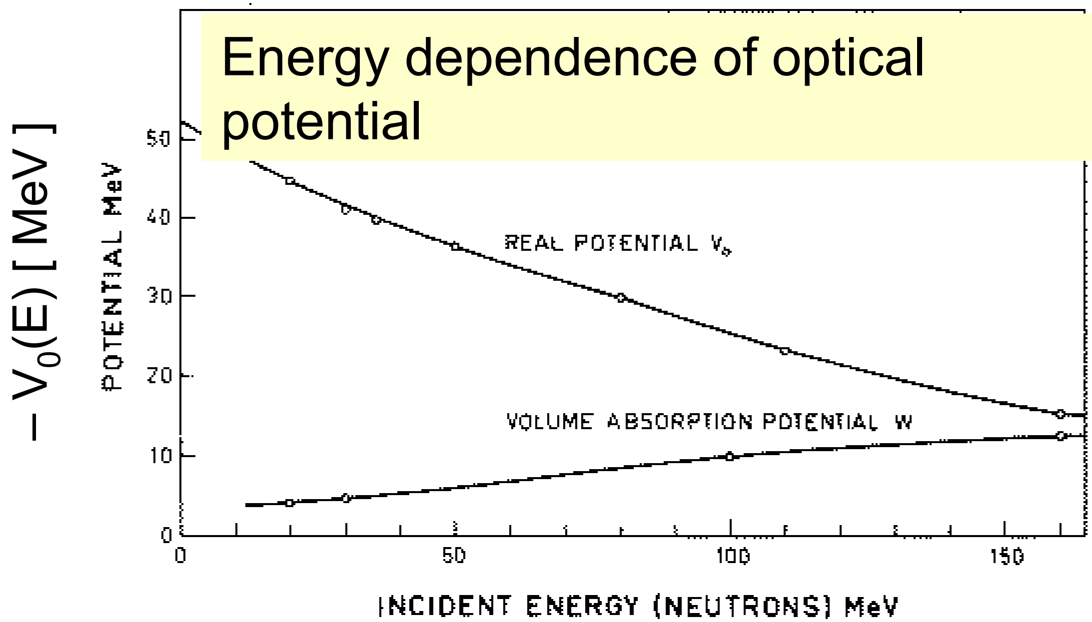

$$V_0 = -52 + 0.3E \text{ [MeV]}$$

$$\frac{m^*}{m} = 1 - \frac{dV_0}{dE} \approx 0.7$$

$$|E - \varepsilon_F| > 20\text{MeV}$$

GQR’s analysis → 0.9~1(?)

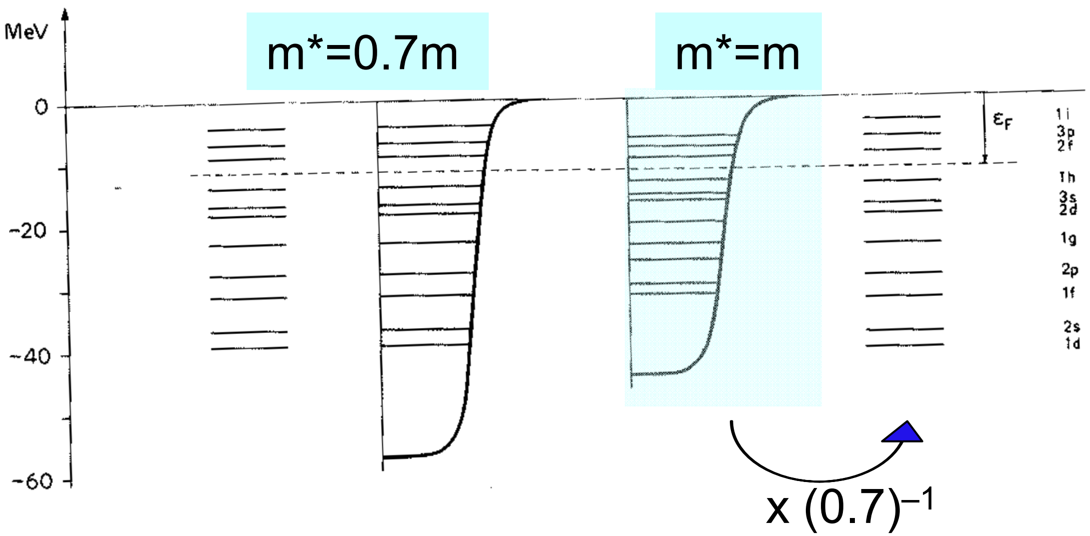

Single-particle level spacings are proportional to m*

Experiments suggest m=m*

$$\frac{m^*}{m} = 1 \quad |E - \varepsilon_F| < 10\text{MeV}$$

Failure of the mean-field models

- In order to explain the nuclear saturation within the mean-field picture, we need an extremely small value of the effective mass.

$$\frac{m^*}{m} = \left(\frac{3}{2} + \frac{5}{2} \frac{B}{A} \frac{1}{T_F} \right)^{-1} \approx 0.4$$

  – This is inconsistent with the experimental data.

- A solution
  – Energy density functional (Rearrangement terms)

$$E[\rho] \Rightarrow \quad h[\rho] | \phi_i \rangle = \varepsilon_i | \phi_i \rangle$$

$$h[\rho] \equiv \frac{\delta E}{\delta \rho}$$

Nuclear energy density functional

- Spin & isospin degrees of freedom
  - Spin-current density is indispensable.
- Nuclear superfluidity → Kohn-Sham-Bogoliubov eq.
  - Pair density (tensor) is necessary for heavy nuclei.

$$E\left[\rho_q, \underbrace{\tau_q}_{\text{kinetic}}, \underbrace{\overleftrightarrow{J}_q}_{\text{spin-current}}; \underbrace{\kappa_q}_{\text{pair density}}\right]$$

$$\Rightarrow \begin{pmatrix} h(t)-\lambda & \Delta(t) \\ -\Delta^*(t) & -\left(h(t)-\lambda\right)^* \end{pmatrix} \begin{pmatrix} U_\mu(t) \\ V_\mu(t) \end{pmatrix} = E_\mu \begin{pmatrix} U_\mu(t) \\ V_\mu(t) \end{pmatrix}$$

Density distribution

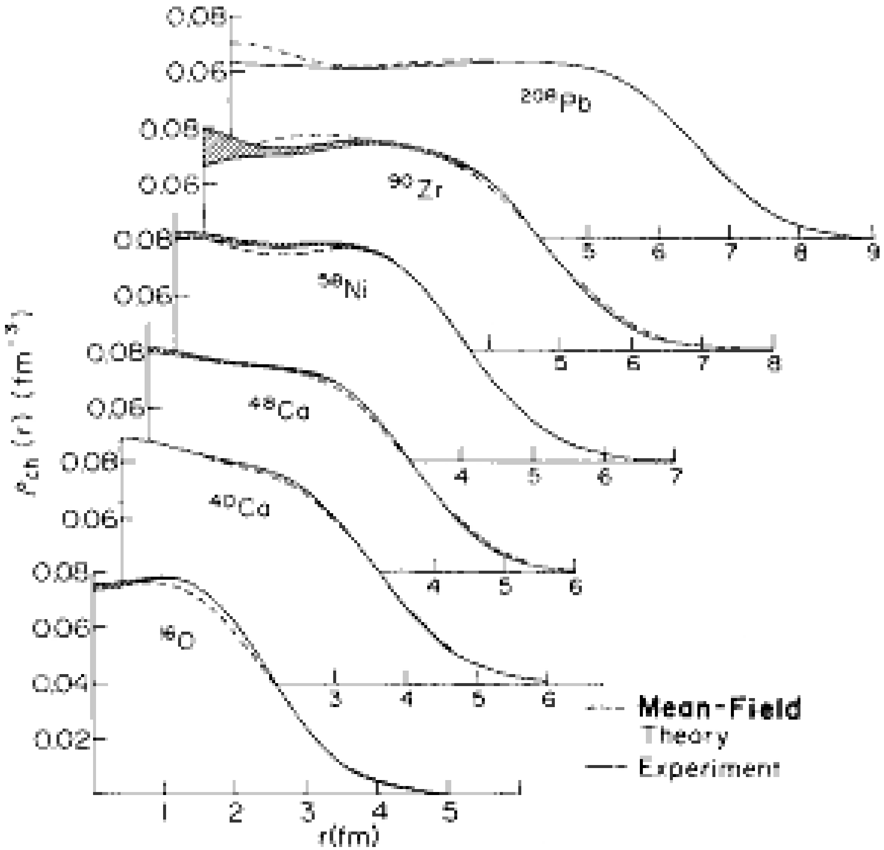

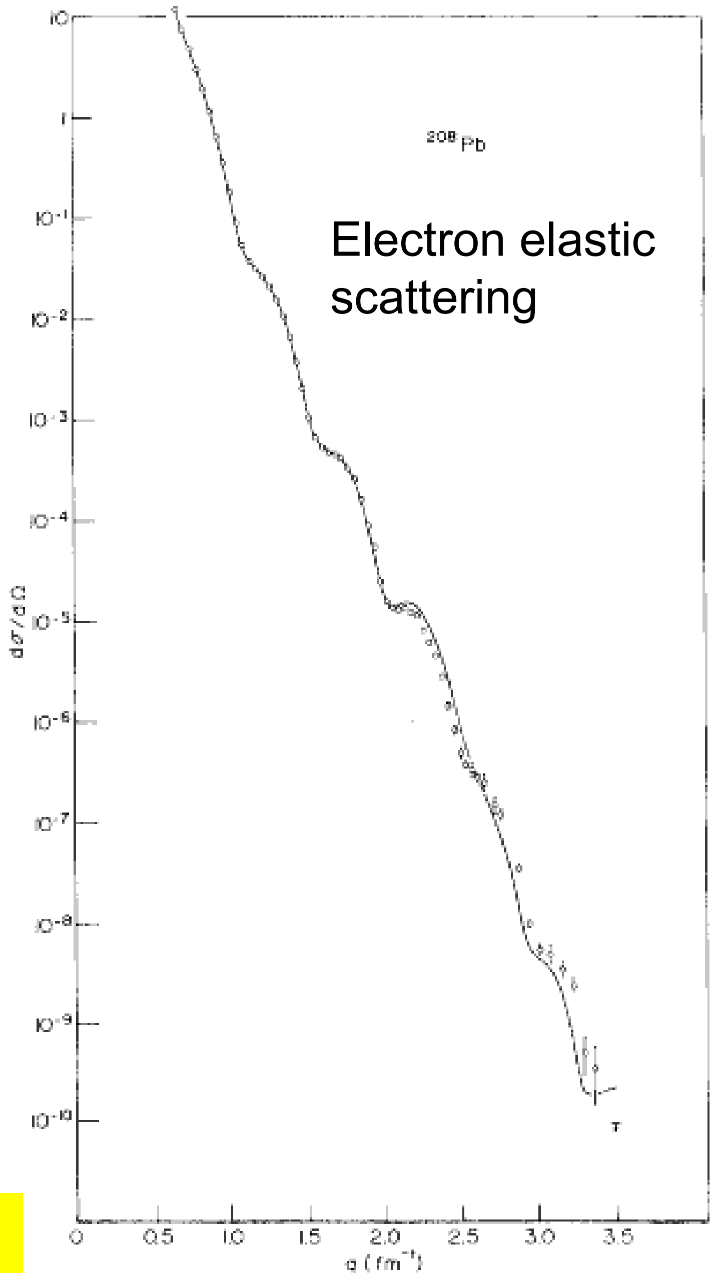

Electron elastic scattering

The strong & complex state-dependence of the effective nuclear interaction is nicely replaced by the Energy density functionals.

Made possible a universal description

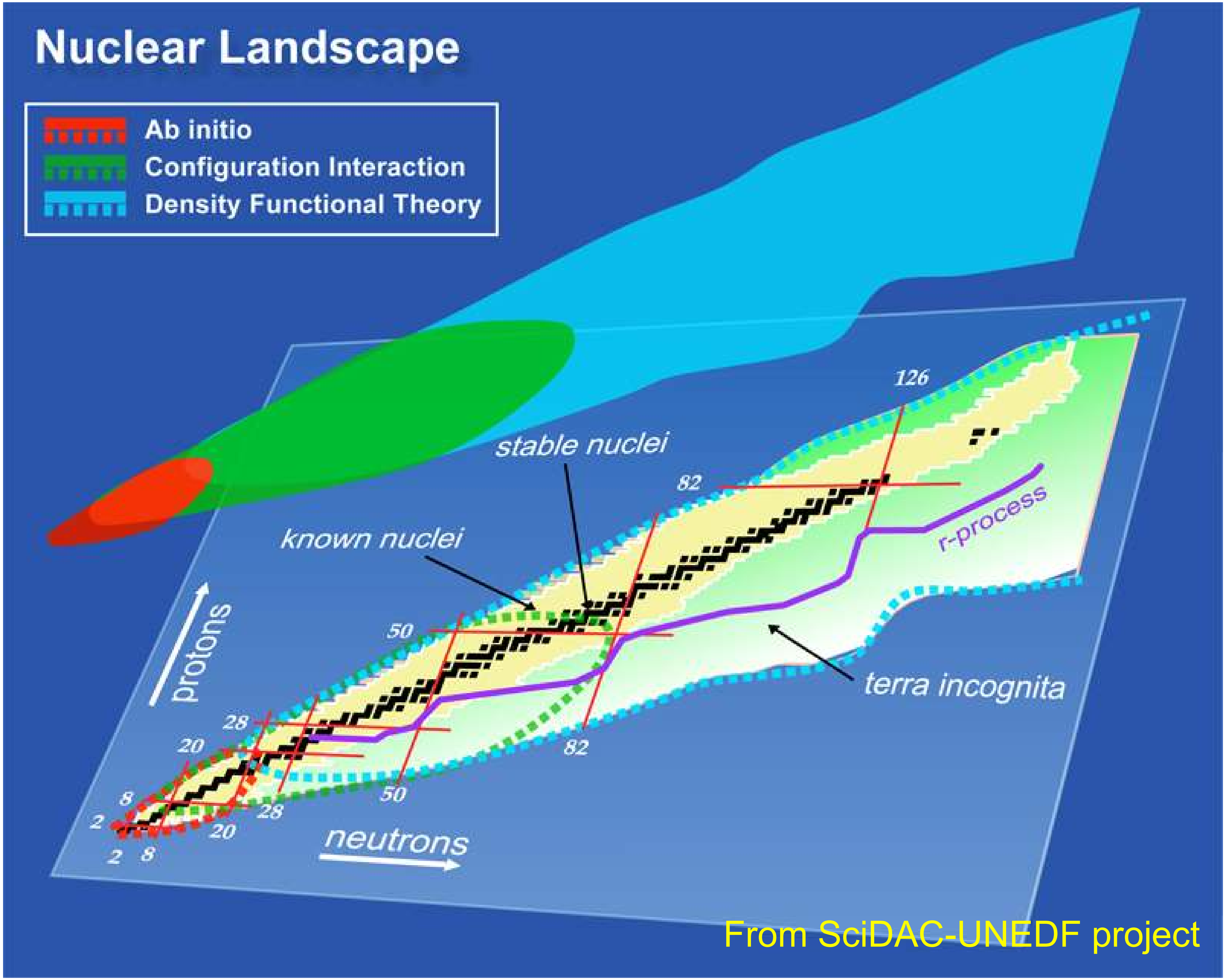
Nuclear Landscape
Ab initio
Configuration Interaction
Density Functional Theory
stable nuclei
known nuclei
terra incognita
r-process
protons
neutrons
126
82
50
28
20
8
2
82
50
28
20
8
2
From SciDAC-UNEDF project

Nuclear deformation as symmetry breaking

$$e^{i\phi J}|\Psi\rangle \neq |\Psi\rangle$$

Quadrupole deformation

$$\beta_{2\mu} = \langle\Psi|r^2 Y_{2\mu}|\Psi\rangle$$

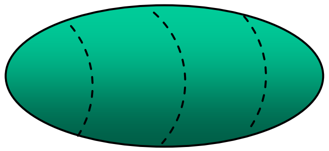

prolate

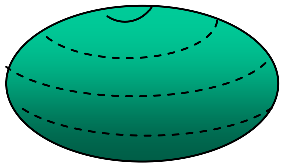

oblate

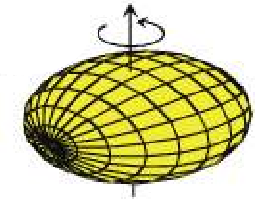

triaxial

Octupole deformation

$$\beta_{30} = \langle\Psi|r^3 Y_{30}|\Psi\rangle$$

$$\hat{P}|\Psi\rangle \neq \pm|\Psi\rangle$$

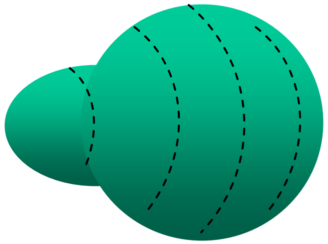

Pear shape (μ =0)

$$e^{i\phi N}|\Psi\rangle \neq |\Psi\rangle$$

Pairing deformation
(superfluidity)

$$\Delta = \langle\Psi|\hat{\psi}\hat{\psi}|\Psi\rangle$$

Deformation in the gauge space

Nuclear Superconductivity
Nuclear Superfluidity

Nuclear deformation predicted by DFT

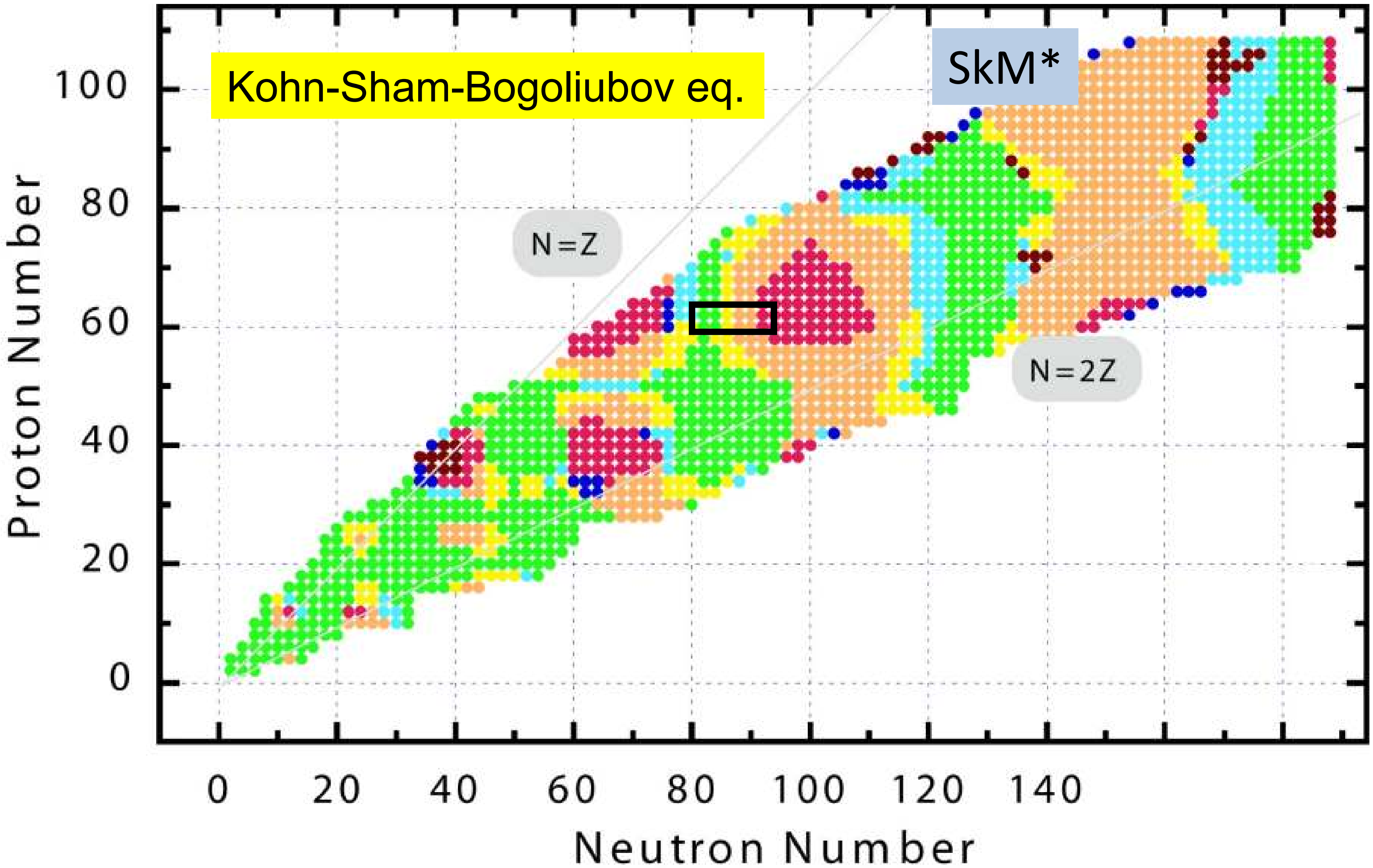

M.V. Stoitsov *et al*., Phys. Rev. C68(2003) 054312

Nuclear deformation is prevalent in the nuclear chart

Nuclear deformation predicted by DFT

Intrinsic Q moment

$\langle \hat{Q}_{20} \rangle$

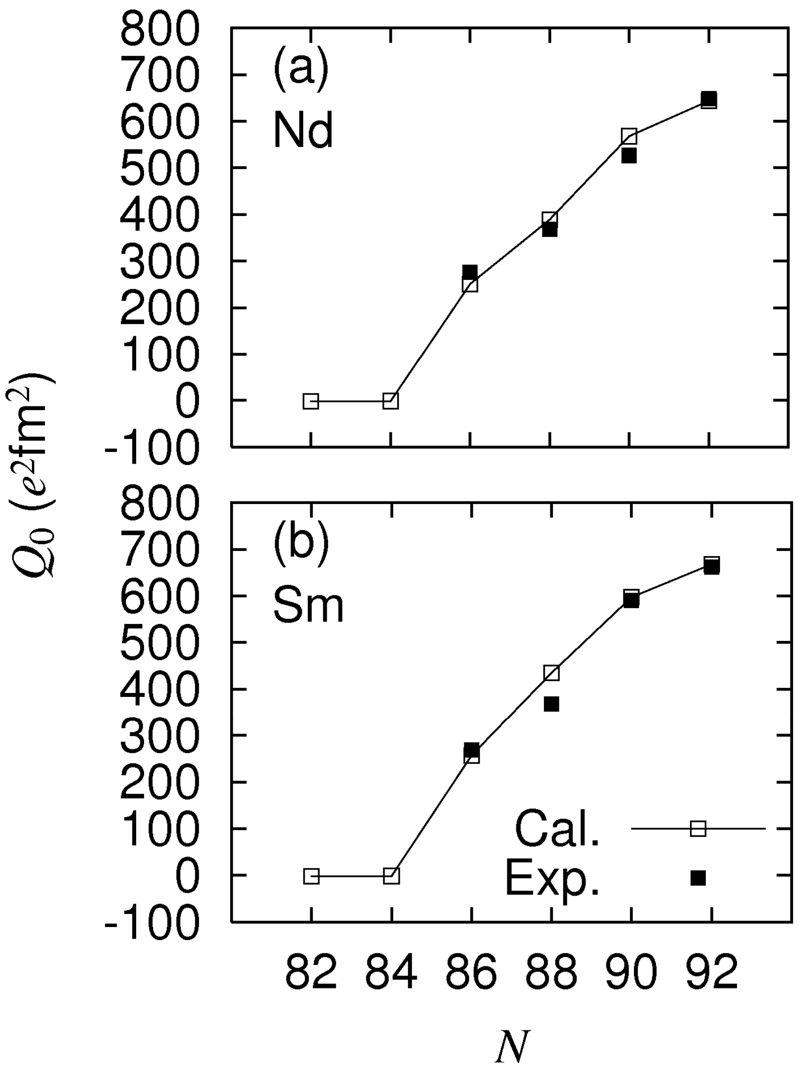

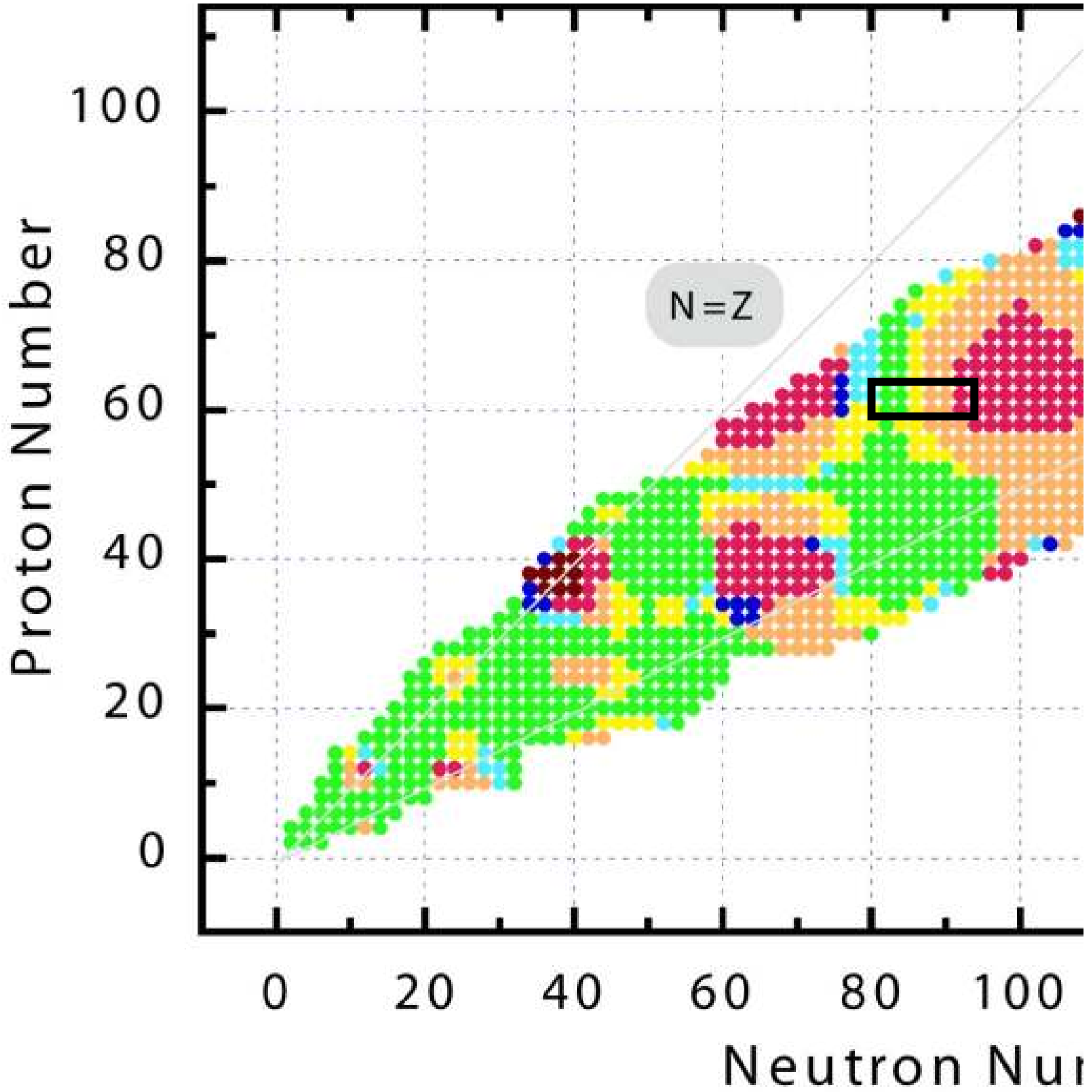

Time-dependent density functional theory (TDDFT) for nuclei

- Time-odd densities (current density, spin density, etc.)

$$E\left[\rho_q(t),\tau_q(t),\overleftrightarrow{J}_q(t),\vec{j}_q(t),\vec{s}_q(t),\vec{T}_q(t);\kappa_q(t)\right]$$

kinetic
spin-current
current
spin
spin-kinetic
pair density

- Time-dependent Kohn-Sham-Bogoliubov eq.

$$i\frac{\partial}{\partial t}\begin{pmatrix} U_\mu(t) \\ V_\mu(t) \end{pmatrix} = \begin{pmatrix} h(t)-\lambda & \Delta(t) \\ -\Delta^*(t) & -\left(h(t)-\lambda\right)^* \end{pmatrix}\begin{pmatrix} U_\mu(t) \\ V_\mu(t) \end{pmatrix}$$

Linear response calculation

Deformation effects for photoabsorption cross section

SkM* functional

K.Yoshida and TN, PRC83, 021404 (2011).

Intrinsic Q moment

$$\langle \hat{Q}_{20} \rangle$$

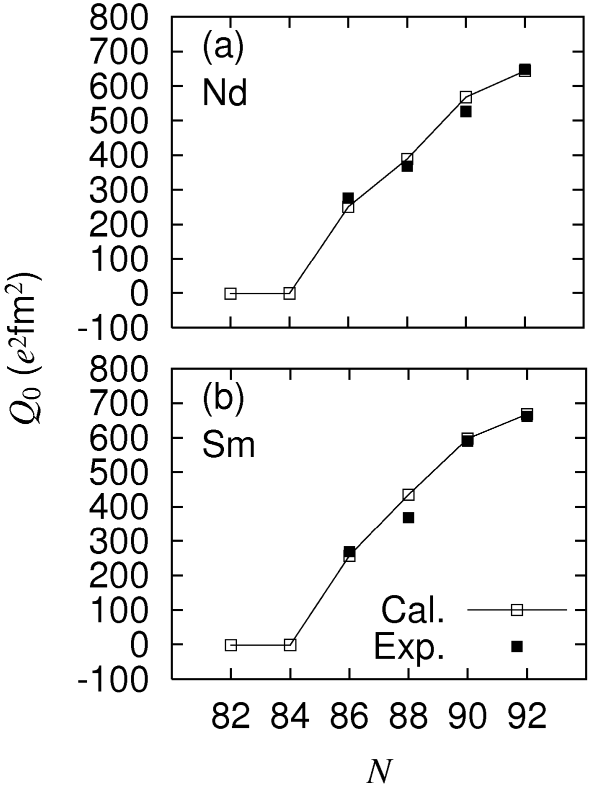

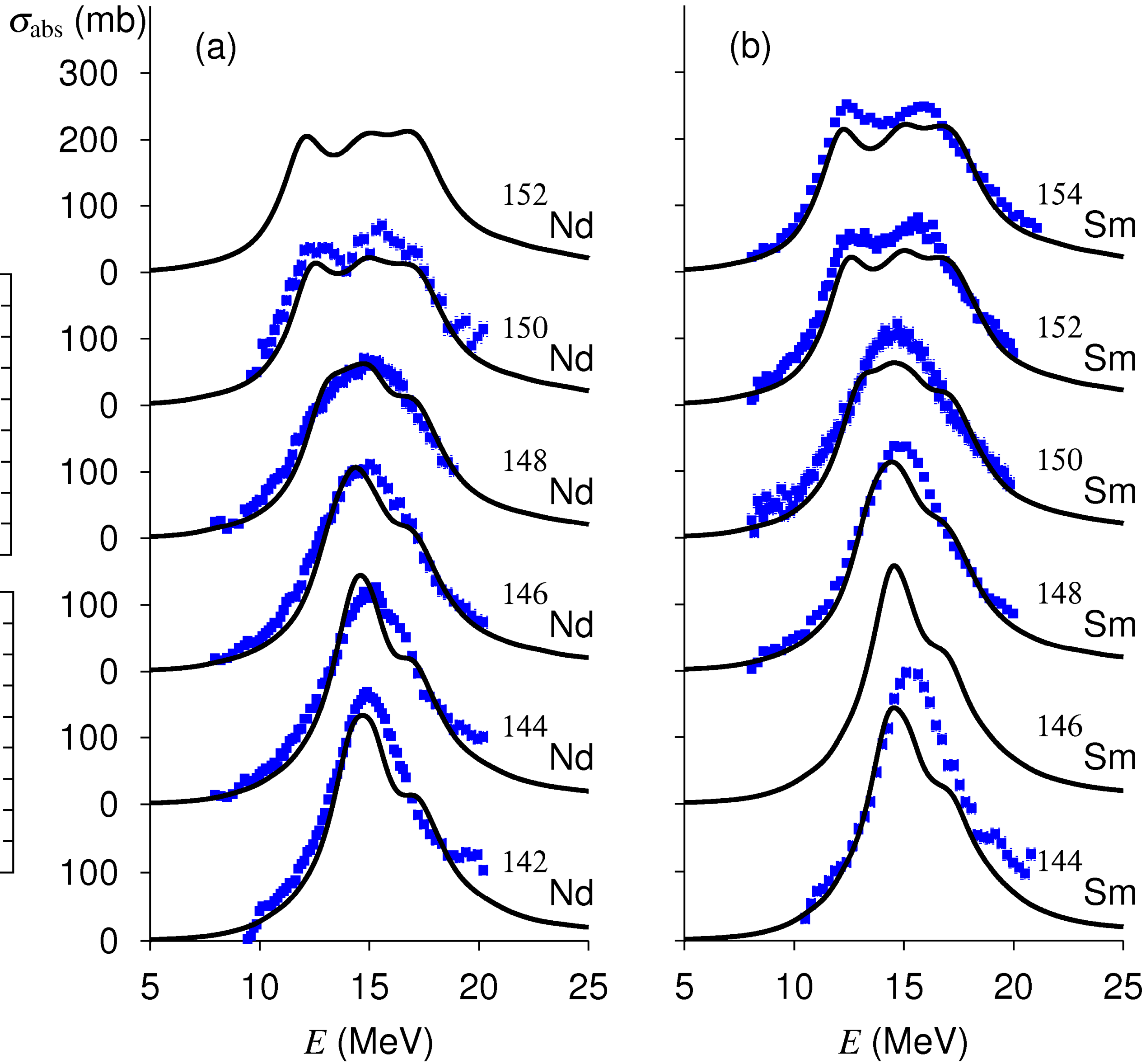

Calculations with HPC

Calculated by K.Yoshida (RIKEN)

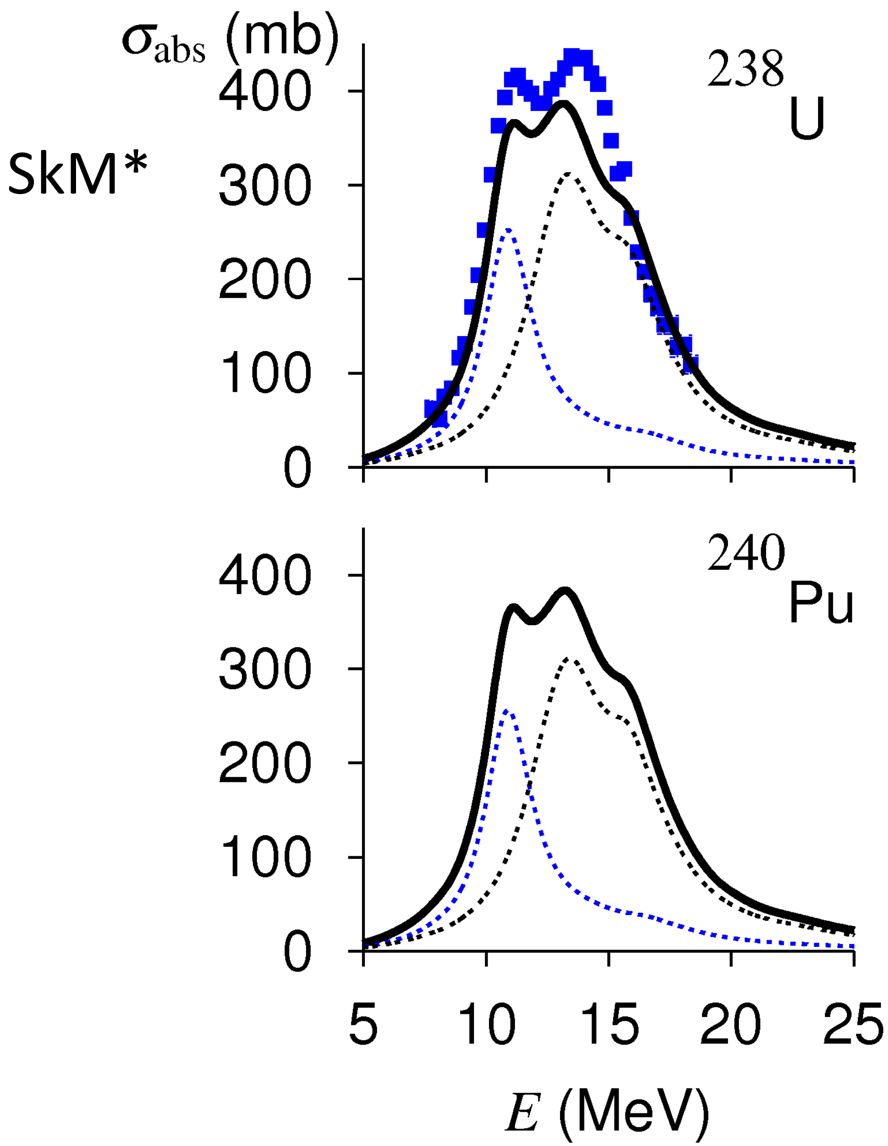

HFB calc. (using 64 CPUs)

Box: $14.7\ \mathrm{fm} \times 14.4\ \mathrm{fm}$

Cut-off: $\Omega \leqq \frac{31}{2},\ E_\alpha \leqq 60\ \mathrm{MeV}$

QRPA calc.

Cut-off: $E_\alpha + E_\beta \leqq 60\ \mathrm{MeV}$

# of 2qp excitation: about 50,000

Matrix elements: 590 CPU hours
Diagonalization: 330 CPU hours

512 CPUs@RICC

Matrix elements: 69 minutes
Diagonalization: 38 minutes

Computational nuclear data tables

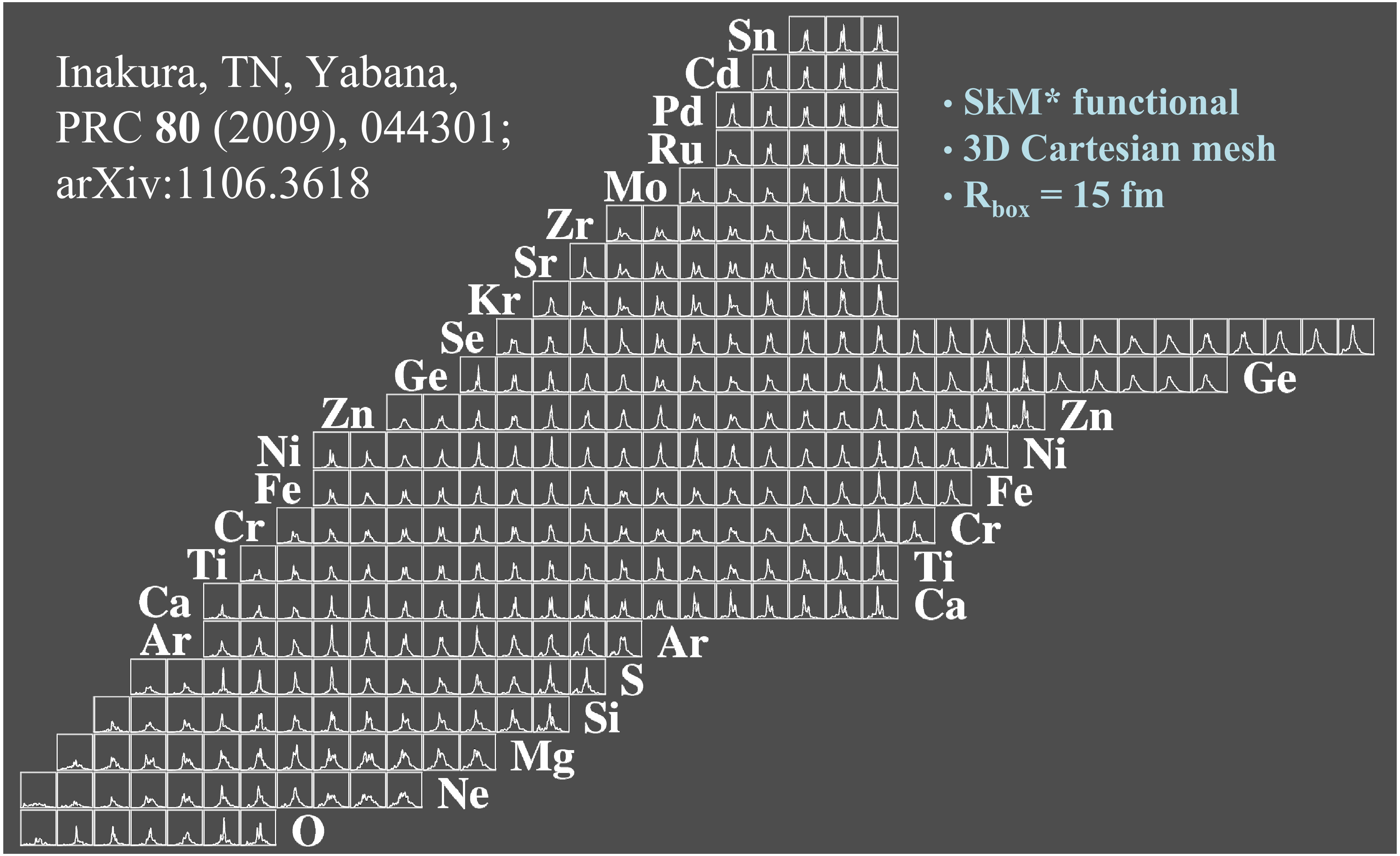

まとめ

- 平均場（独立粒子）描像と原子核の飽和性は相容れない性質をもつ
  - “気体的”・“液体的”性質の統一には、状態に依存する有効相互作用が不可欠（密度依存力）
- エネルギー密度汎関数として統一可能
  - 一粒子運動のKohn-Sham方程式で、密度・エネルギーの飽和性も再現
- 密度汎関数計算
  - 束縛エネルギー・半径・密度分布等の基底状態の性質
  - 対称性の自発的破れによる変形（空間・ゲージ空間）
  - 励起スペクトルの性質
- 将来の課題
  - 奇核のスピン・パリティ、ドリップラインの確定
  - 核融合・分裂などの微視的計算
  - 量子的核反応計算との結合